Astron. Astrophys. 332, 1025–1034 (1998)

ASTRONOMY AND ASTROPHYSICS

A study of the interstellar gas surrounding Carina OB2

J.R. Rizzo[1,⋆] **and E.M. Arnal**[1,2,⋆⋆]

[1] Instituto Argentino de Radioastronomía, C. C. N° 5, 1894 Villa Elisa, Argentina
[2] Facultad de Ciencias Astronómicas y Geofísicas, Av. Paseo del Bosque s/n, 1900 La Plata, Argentina

Received 15 September 1997 / Accepted 8 December 1997

Abstract. A huge HI cavity delimited by a large and ellipsoidal HI feature, has been found toward the stellar association Car OB2. Based on the good agreement found between the mean radial velocity of the HI feature ($V_{HI} \approx -27 \pm 5$ km s^{-1}) and the radial velocity of the OB association ($V_* \approx -33 \pm 8$ km s^{-1}), and the coincidence in position between the barycentral position of the HI feature and the optical position of Car OB2, a physical link between the neutral gas and the stellar association is suggested. The interaction of the stellar winds of the most massive members of Car OB2 with its local ISM could have given rise to both the HI low emissivity region and the surrounding HI shell. The HI shell appears to be expanding at ~ 22 km s^{-1}.

The HI feature has a counterpart in the CO emission. The size and kinematical parameters of the molecular gas almost mimic those of the atomic gas.

Based on the evidence presented in this paper, the anomalous behavior of the HI along $l \approx 290°$, first noticed by Humphreys & Kerr (1974), would merely be a perturbation of the HI local to Car OB2, and would not represent a phenomenon on a galactic scale.

Key words: open clusters and associations: individual: Car OB2 – ISM: clouds – HII regions – ISM: kinematics and dynamics – radio lines: ISM

1. Introduction

Car OB2 $(l, b) \approx (290.^\circ 0, 0.^\circ 4)$ is an extended ($\phi \approx 40$') and rich stellar association located at ≈ 3 kpc from the Sun, in the Sagittarius-Carina arm (García 1993, 1994).

Photographic magnitudes and colours of 480 stars in the field of Car OB2 were determined by Seggewiss (1970). A thorough spectroscopic and photometric study of Car OB2 was undertaken by García (1993, 1994). She derived several global properties of this association, such as its distance (~ 3.1 kpc), its age ($\sim 4\,10^6$ yr), its mean radial velocity (-33 km s^{-1}), its overall mean reddening (0.45 mag) and its luminosity function. Several open clusters present in the region, namely Cr 240, NGC 3572, NGC 3590, Hogg 11 and Tr 18, may be physically related to the association (Clariá 1976). Radial velocities, unless otherwise stated, will always be referred to the LSR.

The most conspicuous HII regions in the field were observed in Hα by Georgelin & Georgelin (1970, 1976), who reported radial velocities around -20 km s^{-1} in most cases; however the HII regions RCW 54a and RCW 54b show Hα radial velocities of ~ 20 and 0 km s^{-1}, respectively. At radio wavelenghts, this direction of our Galaxy has been one of the prime targets of continuum studies performed at 85.5 and 1440 MHz (Mathewson et al. 1962), 408 MHz (Shaver & Goss 1970), 2650 MHz (Thomas & Day 1969) and 5000 MHz (Goss & Shaver 1970). Though at those frequencies several sources of continuum radiation are seen projected close to Car OB2, this angular proximity does not necessarily imply a physical link, for the Sagittarius-Carina arm stretches, at $l = 290°$, along the line of sight. The recombination line surveys of Wilson et al. (1970) in H109α and Caswell & Haynes (1987) in H109α and H110α discovered tens of new HII regions associated with continuum sources. Though most of them have radial velocities ranging from -30 to -10 km s^{-1}, a few were detected at positive velocities. These quite dissimilar radial velocities reflect the line-of-sight effects mentioned above. The large-scale distribution of molecular gas was studied by Grabelsky et al. (1987, 1988), using the J = 1 → 0 ^{12}CO line. Several sources of OH, both in absorption (Caswell & Robinson 1974) and in emission (Manchester et al. 1970, Robinson et al. 1974), disclosed the presence of regions of enhanced gas density.

A large-scale kinematic anomaly in the Sagittarius-Carina arm was reported by Humphreys & Kerr (1974, hereafter HK). This anomaly produces a systematic velocity difference between the stars and the interstellar HI of the order of $\approx$ 10-20 km s^{-1}, in the sense 'gas-star'. The existence of "streaming motions"

Send offprint requests to: José Ricardo Rizzo
⋆ Fellow of the Consejo Nacional de Investigaciones Científicas y Técnicas, CONICET, Argentina
⋆⋆ Member of the Carrera del Investigador Científico of the CONICET

Table 1. Extracted HI and CO surveys

Parameter		Strong et al. (1982) [HI]	Kerr et al. (1986) [HI]	Grabelsky (1986) [CO]
Beamwidth (HPBW)	(arcmin)	16	50	8.8
Sampling interval in l and b	(degrees)	0.5, 1.0	0.5, 0.25	0.125, 0.125
Noise brightness temperature (*rms*)	(K)	0.2	0.05	0.14
Velocity resolution	(km s^{-1})	0.824	1.00	1.3
Velocity coverage	(km s^{-1})	-211 to +161	-350 to +100	-115 to +115

along the spiral arm was suggested as a possible explanation of this phenomenon.

It is known that O type stars emit a copious amount of ionized photons shortwards of the Lyman continuum limit ($\lambda \approx 912$ Å). Thus, the interstellar medium (ISM) close to these massive stars is ionized and photoevaporated by this energetic radiation (Bania & Lyon 1980). Another outstanding characteristic of massive stars is their high mass-loss rate. It may range from 10^{-6} M$_\odot$ yr^{-1} for an O-type star to 10^{-9} M$_\odot$ yr^{-1} for a B7V star (Snow 1982; Howarth & Prinja 1989; Blomme 1990; Vacca et al. 1996). The stellar wind velocity is highly supersonic with respect to the ambient gas; then, a fast moving shock propagates outwards in an already ionized medium. This phenomena give rise to the so called interstellar bubbles (Castor et al. 1975; Weaver et al. 1977; McKee et al. 1984; Koo & McKee 1992). Indeed, around a massive star a region of very low density ($\approx 10^{-3}$ cm^{-3}) and high temperature ($\approx 10^{6-7}$ K) is created. This cavity is initially surrounded by an ionized shell of high density material. As times goes by, the ionization front may get trapped within this shell and its outer parts may start recombining. Thus, this expanding shell may become observable as a neutral (either atomic or molecular) expanding structure.

Since OB stars tend to be grouped in OB associations and open clusters, similar structures to those mentioned above are likely to be formed around them (McCray & Kafatos 1987). From an observational point of view, expanding HI structures were detected around several galactic OB associations, such as Per OB2 (Sancisi 1974), Cep OB3 (Simonson & van Someren Greve 1976), Scorpio-Centaurus (de Geus 1988), Ori OB1b (Chromey et al. 1989) and Ara OB1 (Arnal et al. 1987; Rizzo & Bajaja 1994).

In this paper, the large-scale distribution of both the atomic (as traced by the HI) and the molecular material (as delineated by the CO) are investigated. The main goal of this work is to identify the HI and CO structures likely to be physically associated with Car OB2.

2. Observational material

2.1. Neutral hydrogen

In order to study the large scale HI distribution, the surveys of Strong et al. (1982, hereafter SROM) and the Kerr et al. (1986, hereafter KBJK) were used. Their main characteristics are listed in Table 1.

The HI emission arising from the region delimited by $286° \leq l \leq 294°, -6° \leq b \leq +5°$, and spanning the velocity range $-60 \leq V \leq$ +15 km s^{-1}, was analyzed. A systemic velocity difference between the SROM and KBJK surveys, firstly noticed by Cappa de Nicolau et al. (1988), was found. This velocity offset corresponds to a zero-point displacement on the velocity scale of the SROM's data. As a result of our measurements, we have added 3.8 km s^{-1} (the mean shift found in this region between SROM's and KBJK's profiles) to the SROM's velocities.

2.2. Carbon monoxide

The molecular material was studied using the CO-115 GHz survey of Grabelsky (1986). The relevant observational parameters of this survey are listed in the last column of Table 1.

After a global recognition of the main CO features, we have used the CD-ROM version (NRAO 1992) to analyze them. The original database was convolved to an angular resolution of 0.°5. We have studied the region $287° \leq l \leq 293°$, $-5° \leq b \leq +5°$, along the velocity range $-59.5 \leq V \leq$ +10.7 km s^{-1}.

3. Results

3.1. Neutral hydrogen

In order to identify HI structures likely to be associated with Car OB2, the SROM and KBJK surveys were used to construct $[l, b]$ HI column density (N_{HI}) maps. In doing so the HI was assumed to be optically thin. Thus, the N_{HI} in the velocity interval $[v_1, v_2]$ was computed using the formula:

$$N_{HI} = 1.823\ 10^{18} \int_{v_1}^{v_2} T_b\, dv \quad \text{cm}^{-2} \qquad (1)$$

where T_b is the brightness temperature in K.

In both surveys a striking HI distribution was found in the velocity range $-36 < V <$ -26 km s^{-1}. In Figs. 1a (obtained from SROM) and 1b (derived from KBJK) a region of low HI emissivity is clearly visible at $l \approx 290°$ and $-3° \leq b \leq +2°$. A number of HI maxima appear surrounding the HI minimum.

The contribution of the large scale galactic HI distribution was removed by following the procedure outlined by Rizzo &

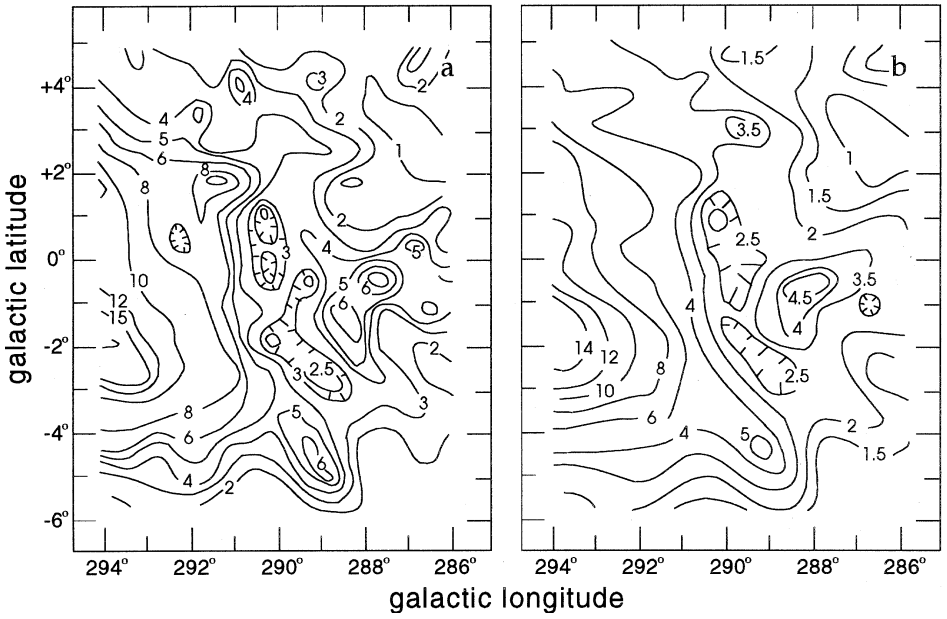

Fig. 1a and b. Neutral hydrogen distribution towards Car OB2, in the velocity range $-36 \leq V \leq -26$ km s^{-1}. Column density contours are in units of 10^{20} cm^{-2}. **a** Survey of Strong et al. (1982). **b** Survey of Kerr et al. (1986)

Bajaja (1994) and fully described by Rizzo (1994). The maps obtained after removing the large scale HI features are called "background-free" maps. A set of these maps are shown in Fig. 2. Each map represents the column density over a 4.8 km s^{-1} velocity interval. An outstanding HI minimum surrounded by an irregular ridge of HI emission, is clearly visible in maps 2c, 2d, 2e and 2f; furthermore, these figures also depicts a set of HI maxima around the hole. At extreme velocities (Figs. 2a, 2b, 2g and 2h) the distribution of the N_{HI} is confined to the central region of each map. In other words, these maps depict a morphology typical of expanding shells: at extreme velocities, the receding (at $V_R \approx$ -45 km s^{-1}) and approaching (at $V_R \approx 0$ km s^{-1}) caps are seen, while at intermediate velocities a ring-like HI structure having a variable radius is observed. If the expanding HI structure is assumed to have spherical symmetry, the ring radius would attain its maximum value at the barycentral velocity of the expanding features. In the case of Car OB2, the HI shell reaches its maximum dimensions at $V_R \approx$ -27 km s^{-1}.

The $[l, V]$ map of the HI distribution (Fig. 3) also shows evidence of an expanding shell. Such figure corresponds to a "background-free" scan at galactic latitude $b = 0°$. There, a central HI hole (or minimum) stands out. The separation between the HI peaks (indicated by a dashed ellipse in Fig. 3) attains its maximum at $V \approx$ -25 km s^{-1}. The walls of surrounding HI merge into a single component at extreme velocities ($\approx$ -50 and -5 km s^{-1}).

Observational parameters of the shell are given in Table 2. The inclination angle refers to the angle made by the major axis of the HI cavity with respect to the galactic plane. The systemic velocity (V_{sys}) was derived as a mean value of the receding ($V_{rec} \approx -5$ km s^{-1}) and approaching ($V_{app} \approx -50$ km s^{-1}) caps of the HI shell. The expansion velocity (V_{exp}) was derived from Fig. 3 as the mean value of $|V_{sys} - V_{rec}|$ and $|V_{sys} - V_{app}|$. These velocities have uncertainties of the order of $\pm$5 km s^{-1}. V_{sys} is found to be forbidden in this direction

Table 2. Parameters of the Carina OB2 HI shell

Parameter	Unit	
Centroid (l, b)	deg	290.1, +0.2
Inclination angle	deg	90
Systemic velocity	km s^{-1}	-27
Expansion velocity	km s^{-1}	22
Major axis[a]	pc	130
Minor axis[a]	pc	80
Mean thickness[a]	pc	20
HI mass[a]	$M_\odot$	1.1 10^5
Total mass[b]	$M_\odot$	1.5 10^5
Mean density[a]	cm^{-3}	~ 1
Kinetic energy[a]	erg	7.1 10^{50}
Expanding momentum[a]	$M_\odot$ km s^{-1}	3.2 10^6
Characteristic lifetime[a]	yr	4.1 10^6

[a] Assuming a distance of 3.1 kpc (see text).
[b] Assuming a mass abundance for the HI of 1.34^{-1}

of the Galaxy (see for example the model of Fich et al. 1989), which reflects the well known deviation of the velocities in the Carina arm toward negative velocities. Bearing these in mind we shall adopt for the HI structure the photometric distance of Carina OB2, namely 3.1 kpc. This distance was used to estimate the lineal size of the HI void and the mean lineal thickness of the shell. Assuming an ellipsoidal distribution for the HI in the expanding structure, both the mass of the shell (M_{sh}) and its mean volume density were derived. By changing the initial conditions imposed to the background substraction method, a mean uncertainty of the order of 40% in the mass determination of the HI shell is expected (Rizzo 1994). Assuming a uniform expansion velocity V_{exp}, the kinetic energy and momentum associated with the expanding material were obtained. Finally, a characteristic lifetime was derived as the ratio of the effective

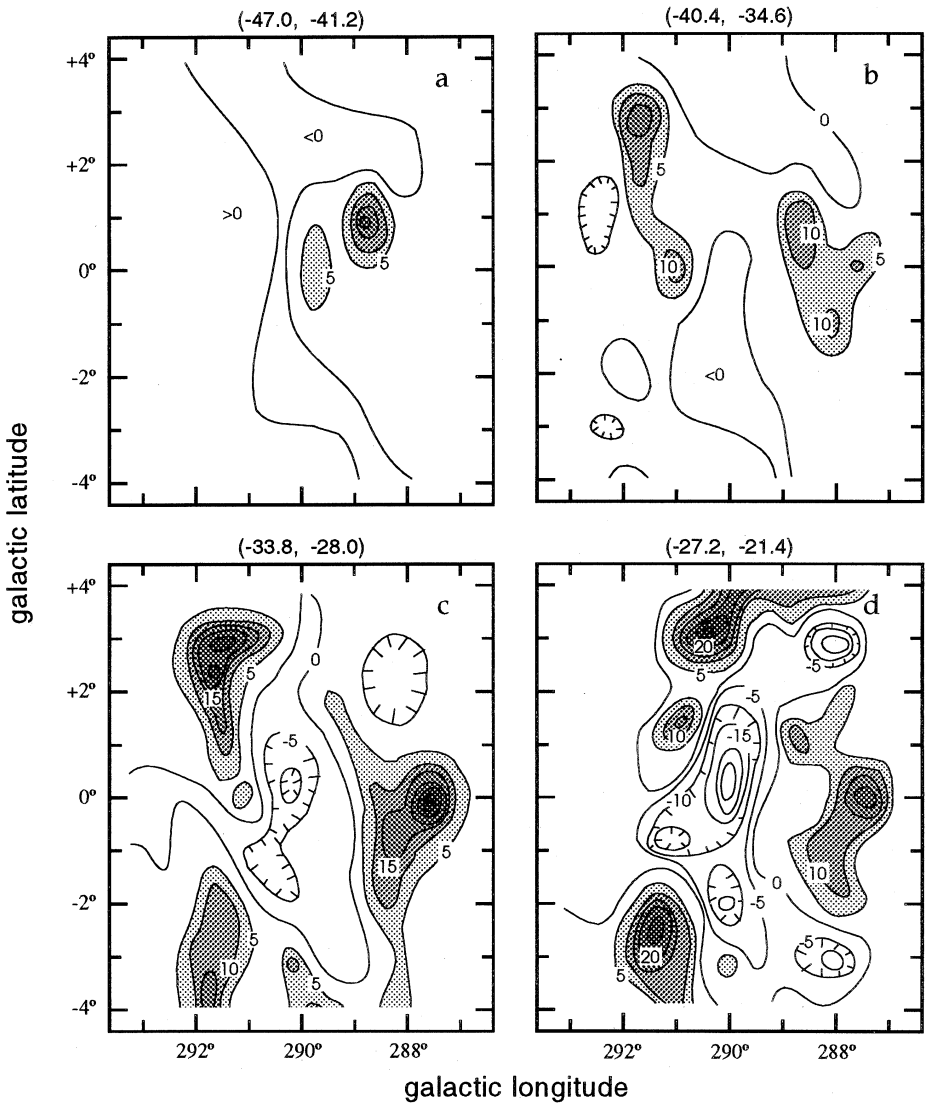

Fig. 2a–h. A series of "background-free" maps in the field of Car OB2 are shown. The velocity intervals are indicated at the top of each figure. Contour levels are in units of 10^{19} cm^{-2}. Hatched areas correspond to emission above the background. These features delineate the expanding structure

radius –the harmonic mean between major and minor axis– and the expansion velocity.

3.2. Carbon monoxide

In order to detect the presence of molecular material in the region under study, we have constructed CO [position-position] and [position-velocity] maps in the velocity range mentioned in Sect. 2.2. In this way, seven molecular complexes of different characteristics (named from A to G) were identified. A brief morphological description of every complex is provided in Table 3.

Fig. 4 shows the CO distribution in the velocity range $-29.6 \leq V \leq -15.3$ km s^{-1}. There, several of the molecular features, namely complexes B, C, D and E, are sketched. Fig. 5 shows a $[l, V]$ map, integrated over $-0.^{\circ}5 \leq b \leq +0.^{\circ}5$. For a later discussion, the HI distribution is drawn in Fig. 5 as dashed contour lines.

4. Discussion

4.1. The shell-like feature surrounding Car OB2 and its possible origin

4.1.1. The HI shell

Based on the results shown in Sect. 3.1, three main conclusions can be drawn. Firstly, there is a minimum in the overall HI distribution towards Car OB2, spanning the velocity range -30 to -20 km s^{-1}. This HI void appears surrounded by an expanding and fragmented shell of neutral hydrogen. Secondly, the centroid of the HI void ($l \approx 290.^{\circ}0, b \approx +0.^{\circ}2$) is almost coincident with the optical center of Car OB2 ($l \approx 290.^{\circ}1, b \approx +0.^{\circ}6$; García 1994). Thirdly, the systemic radial velocity of the HI shell ($V_{sys} \approx -27$ km s^{-1}) is in very good agreement with the mean stellar radial velocity of Car OB2 ($V_* \approx -33$ km s^{-1}). These facts lead us to think of a physical link between the HI expanding feature and the stellar association. However, since a kinematical anomaly is known to exist in this region of the Galaxy (Humphreys & Kerr 1974), we ought to be cautious

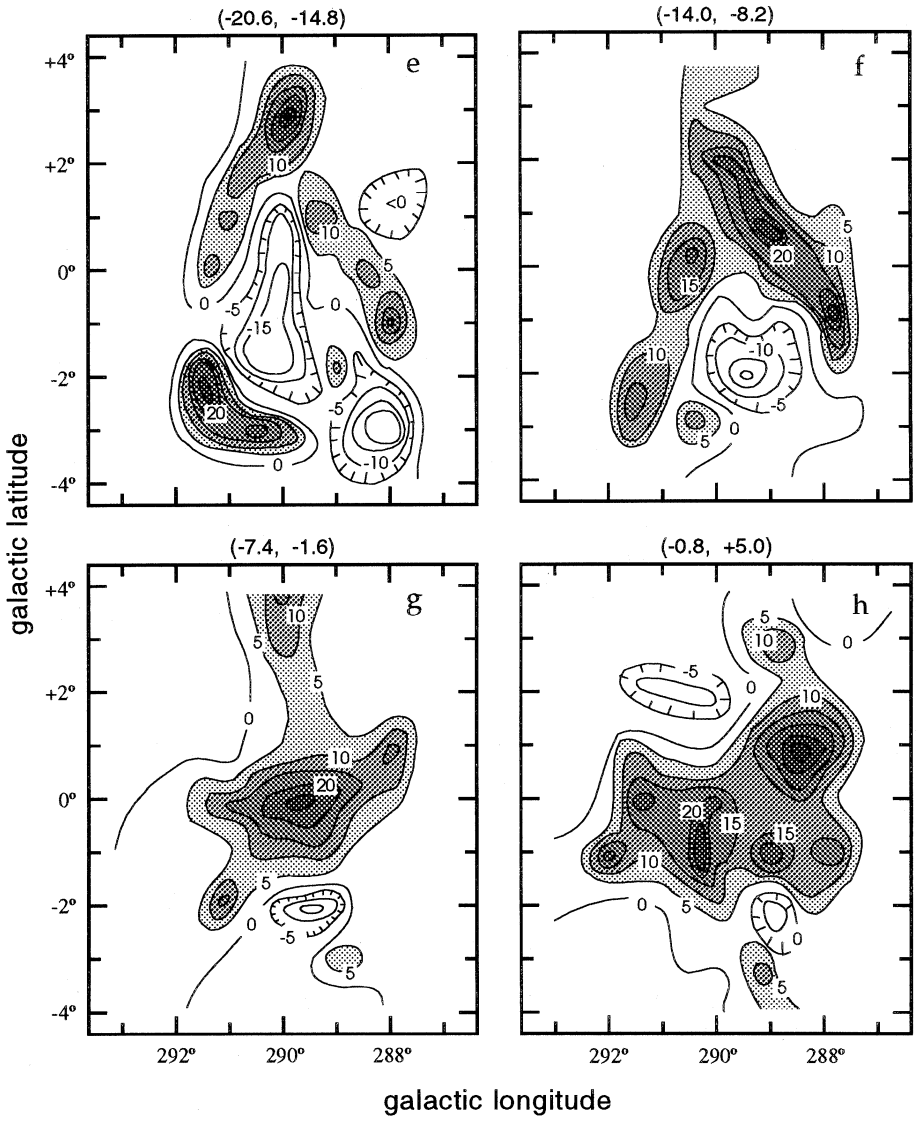

Fig. 2a–h. (continued)

Table 3. Molecular complexes characteristics

Complex	Morphological description	(l, b) extension	Velocity [km s^{-1}]
A	Isolated cloud	(290.°5, +0.°5)	-38
B	Chain of clouds	From (288.°5, +1.°0) to (291.°5, +2.°0)	-36 to -13
C	Arc-shape set of clouds	From (291.°5, -0.°5) to (290.°5, -3.°0)	-28 to -16
D	Extended isolated cloud	(288.°5, -1.°0)	-20
E	Isolated cloud	(292.°5, +2.°0)	-18
F	Nucleus of an extended structure	(291.°0, +0.°0)	-12
G	Massive cloud, 1° in diameter	(290.°5, -0.°5)	-1

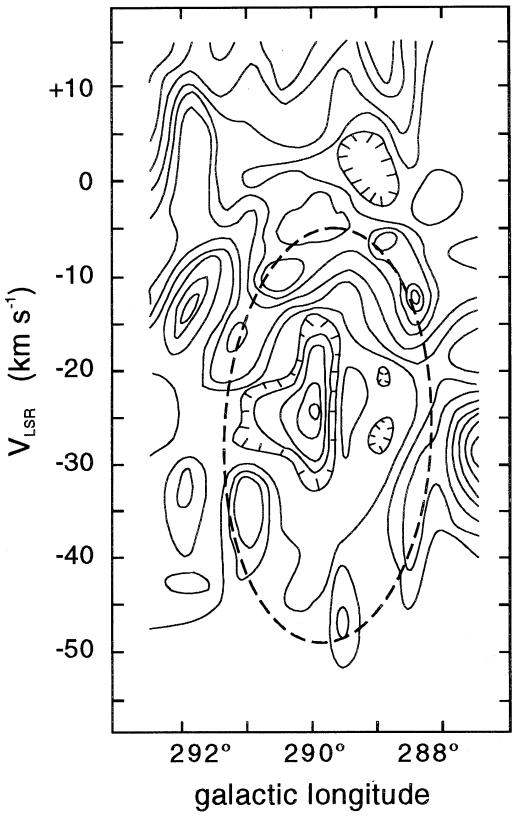

Fig. 3. Galactic longitude-velocity map for $b = 0°$, after subtracting the HI background. The dashed ellipse roughly outlines the positions of the HI maxima that appear surrounding the region of low HI emissivity This arrangement is typical of an expanding structure (see Sect. 3.1)

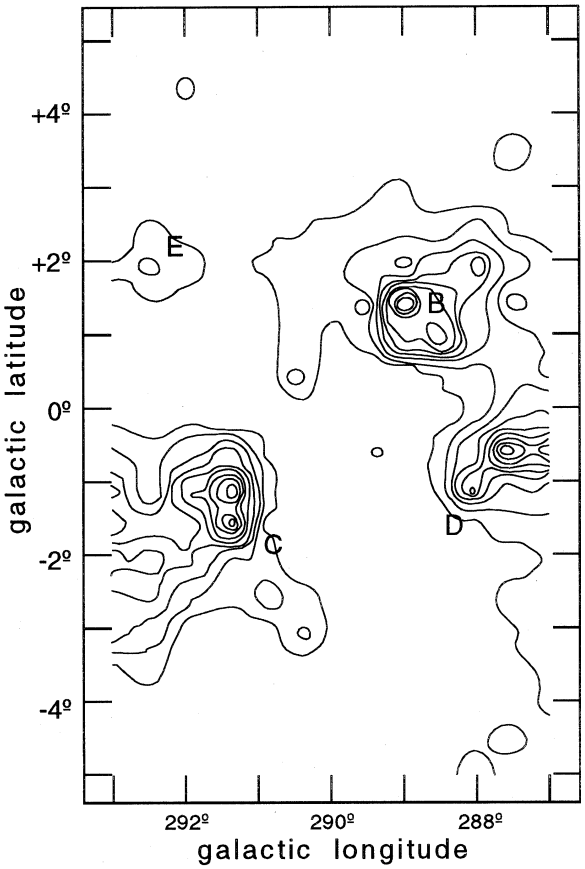

Fig. 4. Distribution of the carbon monoxide (CO) in the vicinity of Car OB2. The velocity range shown here covers the -29.6 to -15.3 km s^{-1} interval. Letters B, C, D and E indicate the position of the molecular complexes identified in Sect. 3.2.

in interpreting the velocity agreement as a strong evidence in favour of a physical association.

When looking for evidences favouring a physical link between the HI shell and the stellar association, both the morphology and kinematics of the HI structure must be taken into account. As mentioned in Sect. 1, UV radiation, stellar winds and SN explosions from the most massive members of Car OB2 could have injected a considerable amount of energy and momentum into the ISM.

Based on the known stellar population of Car OB2 (García 1993, 1994) a rough estimate of the energy injected as winds, by the stars of Car OB2 into its local ISM, can be obtained. Unfortunately, spectral classification is only available for 57 out of the total of 157 stars that are listed as members and probable members by García (1993). In order to evaluate the mass-loss rate and the wind terminal velocity of a given star, a rough knowledge of its spectral type is needed. Thus, to include those stars lacking a spectral classification, we have used for them the intrinsic colors and absolute magnitudes derived by García (1993). From there, and adopting the Schmidt-Kaler (1982; hereafter called SK) calibrations, a spectral type was obtained. We shall call this spectral type a "derived" one. The reliability of this procedure was tested by applying it to those 57 stars that have an observed spectral type. The "derived" spectral types for these 57 stars were compared to their observed ones. All but two stars were classified with their correct luminosity class. Furthermore, the difference in spectral classification was at most one spectral subtype. Based on this agreement, the whole sample of 157 stars was used to estimate the total amount of mechanical energy injected by the stars of Car OB2 into its local ISM. The individual stellar luminosity (L_*) and effective temperature ($T_{\rm eff}$) were derived using the calibrations of SK. These parameters were then used to obtain individual mass-loss rate ($\dot{M}$) and terminal wind velocity ($V_{\rm w}$) by means of the formulae:

$$\dot{M} = 2 \times 10^{-13} L_*^{1.25} {\rm M}_\odot \ {\rm yr}^{-1} \quad (2)$$

and

$$\log V_{\rm w} = -35.2 + 16.23 \log T_{\rm eff} - 1.7 \ (\log T_{\rm eff})^2 \ {\rm km \ s}^{-1} \quad (3)$$

given by Van Buren (1985; VB), which are valid for O and B stars of all luminosity classes. These relations are consistent with those for O stars (Howarth & Prinja 1989) and B stars (Snow 1982). When compared to those estimate given by Blomme & van Rensbergen (1988) and Blomme (1990), the formulae of Van Buren (1985) provide lower limits. With these

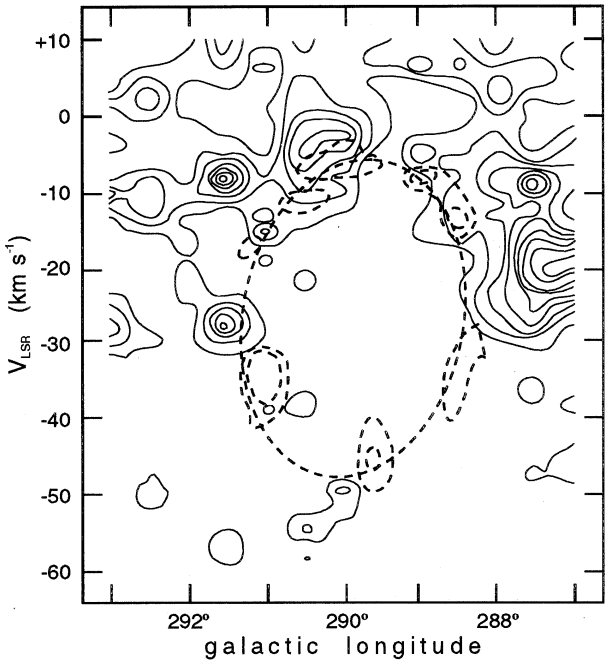

Fig. 5. Galactic longitude-velocity map of the CO in the Car OB2 region, for galactic latitude $-0.^\circ5 < b < +0.^\circ5$. The HI distribution is shown as dashed contour lines

values of $\dot{M}$ and $V_{\rm w}$ the kinetic energy input ("mechanical luminosity", $L_{\rm mech} = \frac{1}{2}\dot{M}V_{\rm w}^2$) and momentum ($\dot{P} = \dot{M}V_{\rm w}$) for every individual star of the sample was derived. Since stars of spectral type later than B2 have a negligible contribution to the injected amount of $L_{\rm mech}$ and $\dot{P}$, we have taken only into account stars of earlier spectral types. In Table 4 the results of this estimate for the stars having spectral types earlier than B2, 24 in total, are given. The supergiants HD 96248 and HD 96261 (also members of Car OB2) were not included in this sample. The first column corresponds to the star number (according to García 1993), the second to the HD number, the third to the spectral type and the fourth, fifth, sixth and seventh columns to the mass-loss rate, wind velocity, mechanical luminosity and momentum rate, respectively. By adding up the individual contribution of these 24 stars, a total mechanical luminosity and momentum loss rate of about $8.0\,10^{36}$ erg s^{-1} and $1.0\,10^{-2}$ M$_\odot$ km s^{-1} yr^{-1}, respectively, are obtained.

With these parameters, the earliest stars of Car OB2 may have injected into the ISM along their lives ($\sim 4\,10^6$ yr), about $1.0\,10^{51}$ erg of mechanical energy and $4.0\,10^4$ M$_\odot$ km s^{-1} of momentum. Using these values and those for the HI shell given in Table 2 to compute both the ratio of kinetic energy of the shell to the injected total wind energy (ϵ_s) and the ratio of momentum of the shell to that imparted by the wind (π_s) (McCray 1982), we obtain $\epsilon_s \approx 0.7 \pm 0.5$ and $\pi_s \approx 80 \pm 40$, respectively. The quoted uncertainty in both ϵ_s and π_s are formal errors derived under the assumption of 40%, 25%, 200% and 30% uncertainty in the adopted values of M_{sh}, V_{exp}, $\dot{M}$ and $V_{\rm w}$, respectively. It ought to be said that both ϵ_s and π_s are strongly dependent on the contribution made by the O-stars. Thus, it would not be surprising that by adopting for these stars a different calibration for $T_{\rm eff}$, e.g., that of Vacca et al. (1996), and a set of different equations for relating both $\dot{M}$ and $V_{\rm w}$ to $T_{\rm eff}$, e.g., that of Lamers & Leitherer (1993; LL) for $\dot{M}$:

$$\log \dot{M} = 1.738 \log L_* - 1.352 \log T_{\rm eff} - 9.547 \quad (4)$$

and Leitherer et al. (1992; LRD) for V_w:

$$\log V_{\rm w} = 1.23 - 0.30 \log L_* + 0.55 \log M_* + 0.64 \log T_{\rm eff} \quad (5)$$

different values for ϵ_s and π_s are obtained, namely $\epsilon_s \approx 1.4 \pm 0.9$ and $\pi_s \approx 310 \pm 150$.

Owing to the large value of π_s in both cases, one may argue that the HI shell found around Car OB2 is part of an expanding interstellar bubble that is observed in its energy-conserving phase.

Nonetheless, were this the case, the kinetic efficiency turns out to be higher than the theoretical value of $\epsilon_s = 0.2$ (Weaver et al. 1977, McCray 1982, Van Buren 1986). Certainly, the value of both efficiencies are upper limits for we have not included the contribution of the blue supergiants (BSG) HD 96248 and HD 96261 during their main sequence lifetime. Both stars are believed to belong to the Car OB2 association (García 1994).

Under the assumption that no massive star of Car OB2 have undergone a supernova explosion, and since no Wolf-Rayet (WR) star is known to be related to Car OB2, following Schaller et al. (1992) both BSG should came from main sequence progenitors in the mass range 45 to 60 M$_\odot$. This mass range correspond to spectral types O5.5V-O6V. Using the SK $T_{\rm eff}$ calibration and the VB formulae (Eqs. 2 and 3), the total contribution of these two stars along their main sequence lifetime are $\approx 1.5\,10^{51}$ erg of kinetic energy and $4.6\,10^4$ M$_\odot$ km s^{-1}of angular momentum, respectively. Using the Vacca et al. (1996) $T_{\rm eff}$ calibration and the formulae of LL and LRD (Eqs. 4 and 5), the above values are $\approx 7.9\,10^{50}$ erg of kinetic energy and $1.3\,10^4$ M$_\odot$ km s^{-1} of angular momentum, respectively. Thus, following SK and VB, ϵ_s and π_s are 0.3 ± 0.2 and 37 ± 20, respectively; and following LL and LRD, ϵ_s and π_s are 0.6 ± 0.4 and 130 ± 60, respectively.

The physical reality, stellar content and observational parameters of the stellar clusters lying along the direction $l \sim 290^\circ$ have been studied by Walborn (1973), Moffat & Vogt (1975), Clariá (1976) and Steppe (1977). Individual stars have also been observed by Humphreys (1972), Lodén et al. (1976) and Klare & Neckel (1977). The cluster NGC 3572 (= NGC 3572b), located at a distance of 2.7-2.9 kpc (Clariá 1976), appears as the only one that may be physically related to Car OB2. The massive stars of this cluster, seen in projection close to the geometrical center of the HI cavity, might have played a role in originating the expanding motion nowdays observed. The earliest stars of this cluster could have injected to the ISM as much as $2.3\,10^{51}$ erg of mechanical energy and $7.3\,10^4$ M$_\odot$ km s^{-1} of momentum. These values were derived using the SK calibration and Eqs. (2) and (3). Using the calibration of Vacca et al. (1996) and Eqs. (4) and (5) the injected momentum are lower by a factor of ~ 1.9 and ~ 3.3, respectively. Including the possible

Table 4. Earliest stars of Car OB2

Star[a]	HD/HDE	ST	$\dot{M}$ 10^{-6} $M_\odot$ yr^{-1}	V_w km s^{-1}	L_{mech} 10^{36} erg s^{-1}	$\dot{P}$ 10^{-3} $M_\odot$ km s^{-1} yr^{-1}
2		B1.5Ve	0.02	1840	0.02	0.04
8		B1V	0.04	2020	0.05	0.07
21	305938	B1V	0.04	2020	0.05	0.07
89	305982	B0V	0.16	2490	0.32	0.39
180	96622	O9.5V	0.25	2580	0.53	0.64
193	96670	O7V(f)n	1.20	2980	3.40	3.50
227	306035	B1V	0.04	2020	0.05	0.07
231		B0V*	0.16	2490	0.32	0.39
238		B1V	0.04	2020	0.05	0.06
243		B2IV	0.02	1570	0.02	0.37
244		B1.5V	0.02	1680	0.02	0.03
245		B1V	0.04	2020	0.05	0.06
246		B0.5IV	0.17	2190	0.26	0.36
248	96638	O8V	0.69	2860	1.80	2.00
275	96669	B1II-III	0.22	1790	0.22	0.39
276		B1IV	0.07	1950	0.09	0.14
297	96286	B1II-III	0.22	1790	0.22	0.39
309		B1V	0.04	2020	0.05	0.07
314	96159	B1II-III	0.22	1790	0.22	0.39
331	305941	B2IV-V	0.02	1610	0.01	0.03
334	96158	B2II-III	0.11	1420	0.07	0.16
335		B1V	0.04	2020	0.05	0.07
356		B1V	0.04	2020	0.05	0.07
400	96415	B2III	0.04	1480	0.03	0.06

[a] From García 1993
* Spectral type 'derived' in this paper (see text)

contribution of NGC 3572 into the overall energy and momentum budget, the new values of ϵ_s and π_s are $\epsilon_s \approx 0.15 \pm 0.1$ and $\pi_s \approx 20 \pm 10$ in the first case (SK and VB), and $\epsilon_s = 0.2 \pm 0.15$ and $\pi_s \approx 70 \pm 30$ in the second case (LL and LRD).

Summing up, there are strong observational arguments favouring a physical link between the HI shell and the association Car OB2. According to our estimations, the stellar winds of the most massive members of Car OB2 and (very probably) the neighbor cluster NGC 3572b could have injected to the local ISM the necessary energy and momentum to form the features observed in the neutral gas at 21 cm.

4.1.2. The molecular material

In Fig. 4 we can see complexes B, C and D lying close to the elliptic distribution depicted by the HI shell in Figs. 2d and 2e. Furthermore, it is evident from this figure that CO emission is absent from its central region. This lack of material is clearly correlated with the HI cavity (see Fig. 3). Finally, complexes A and G are almost coincident with both "caps" of the HI shell at their corresponding velocities (see Figs. 2a and 2b for complex A, and Figs. 2g and 2h for complex G). Complex F is also projected near one of the maximum of the shell, in Fig. 2f. Complexes A, F and G are not shown in Fig. 4 to avoid an excessive confusion when looking at it.

The spatial correlation between CO and HI is quite clear in Fig. 5, where the maxima of both HI (dashed contours) and CO (solid lines) are shown. This figure seems to support a possible link between the CO and HI. Indeed, by assuming the CO complexes belong to a single expanding feature, its barycentral and expansion velocities turned out to be -20/-25 and 20/22 km s^{-1}, respectively. Assuming a distance of 3 kpc, we derive a lineal radius of $\approx$ 100 pc and a characteristic time of $\approx 5.5\,10^6$ yr. Though it is very hard to establish the uncertainties of these values, they are very similar to those given in Table 2 for the HI shell.

This correlation would imply a common origin for both atomic and molecular expanding gas, but we ought to be cautious in considering the amount of molecular mass that is actually participating from the expanding motion.

4.2. The "kinematic anomaly" in the Carina arm

4.2.1. An alternative explanation

In a classical paper, HK have compared the radial velocities of both field supergiant stars and stars embedded in HII regions with those of the neutral hydrogen gas at $289° \leq l \leq 291°$. Defining the velocity residual as $V_{res} = V_{obs} - V_{mod}$, where V_{obs} is the observed radial velocity and V_{mod} is the radial velocity

derived from the Smith (1965) model, they concluded that the supergiant stars show negative velocity residuals, while all of the stars in the HII regions have positive residuals.

A similar behaviour was noticed for the HI, where the distribution at $288\overset{\circ}{.}5 \leq l \leq 290\overset{\circ}{.}5$ show the high HI temperature contours shifted toward positive velocities with respect to the supergiant radial velocities. This effect was not present when a similar comparison was made at both $l \leq 288^\circ$ and $l \geq 291^\circ$. They also mentioned that the HII regions show a good agreement in velocity with the neutral gas. The observed positive velocity shift of the HI is of the order of 10 - 20 km s^{-1}. According to HK, the region showing this anomalous HI gas motion is centered around $l \approx 289\overset{\circ}{.}5$, extends over 2° in longitude and its extent in latitude is at least 4°. We shall refer to this anomalous HI motions as to the "neutral hydrogen anomaly" (hereafter referred to as the NHA).

At this point, bearing in mind the parameters observed for the Carina HI shell (see Table 2), it is unavoidable to conclude that they almost mimic those quoted by HK for the NHA. Thus, we believe that the "neutral hydrogen anomaly" of HK reflects the action of the early type stars of Car OB2 on its surrounding ISM. From our point of view, the NHA is a phenomenon local to Car OB2 and does not represent a large scale phenomenon along the Carina spiral arm.

In this context, the gas shifted by 10 - 20 km s^{-1} toward positive velocities could be identified with the receding part of the HI shell, $V_{rad} \approx$ -5 km s^{-1}, whilst the gas seen at -50 km s^{-1} (see Fig. 11 of Grabelsky et al. 1987) could be identified with the approaching HI cap.

4.2.2. Sequential star formation in Car OB2?

In this section we would like to draw the attention of the reader towards one point, admittedly highly speculative, which may be worth to pursuing further. The HII regions RCW 54b, RCW 54d and RCW 55 have distances comparable to the distance quoted for the HI shell associated with Car OB2, and all of them are seen in projection onto the same sky area where the HI expanding shell is observed.

By assuming a very crude model for the expanding HI structure, namely a spherically symmetric shell having as radius the geometric mean of the major and minor axis, the centroid and both the barycentral and the expansion velocities listed in Table 2, namely R = 100 pc, $(l, b) = (290\overset{\circ}{.}1, +0\overset{\circ}{.}2)$, $V_{sys} = -27$ km s^{-1} and $V_{exp} = 22$ km s^{-1}, respectively, a model radial velocity of -7 (-5.6), -12.3 (-13.0) and -22 (-10.9) km s^{-1} are obtained for RCW 54b, RCW 54d and RCW 55, respectively. The numbers in bracketts indicate the mean of the observed radial velocities, as quoted in the paper of HK. The HII regions are assumed to be located in the receding part of the HI structure. Except for RCW 55, for which even this simple model is certainly an oversimplification, the "model radial velocities" are in reasonable agreement with the observed ones.

Based on the above, we may interpret RCW 54b, RCW 54d and RCW 55 as a bunch of HII regions that may be physically related to the receding part of the HI expanding structure, as opposed to the view that they represent HII regions stretching along the line of sight to Car OB2 lying between 2.4 and 3.7 kpc from us. Were our interpretation correct, these HII regions would represent another example of sequential star formation in our Galaxy.

5. Conclusions

Two HI-21 cm surveys were used to study the distribution of the atomic gas, as traced by the HI, towards Car OB2. As a complement, CO-115 GHz observations were used to investigate the molecular gas in the same region. The main findings of this study are the following:

1. A large region with a low HI emissivity was found projected onto Car OB2. The centroid of this HI void is almost coincident with the optical position of the stellar association. The radial velocity range in which this HI cavity appears is in very good agreement with the mean radial velocity of Car OB2, namely -33 km s^{-1}. We believe the HI shell is physically linked to Car OB2.
2. Based on "background-free" maps, both the kinematics and morphology of the HI shell were studied. The Car OB2 HI shell, centered at $(l, b) \sim (290\overset{\circ}{.}1, +0\overset{\circ}{.}2)$, has a total (assuming solar abundances) atomic gas mass of $\approx 1.5\,10^5$ M$_\odot$ and a barycentral radial velocity of -27 km s^{-1}, which is forbidden in this direction of the Galaxy. The overall structure is expanding with a velocity of 22 km s^{-1}. The shape of this HI feature is ellipsoidal, with a major axis of ~ 130 pc almost perpendicular to the galactic plane. The axial ratio of this structure is ~ 1.7. The HI shell is assumed to be at the photometric distance of Car OB2, namely 3.1 kpc.
3. There is a striking spatial correlation between the atomic gas, as traced by the HI, and the molecular material, as traced by the CO emission. The molecular material depicts both a spatial and kinematical distribution that is in very good agreement with that of the HI.
4. The mechanical power injected by the most massive stars of Car OB2 alone, by means of their stellar winds, could be the origin of the observed expanding HI structure. The most massive stars of NGC 3572b may also have played a role in its genesis.
5. An alternative explanation for the anomalous behaviour of the HI along the line of sight to Car OB2, first noticed by Humphreys & Kerr (1974), is given. According to our interpretation, the complex HI velocity field observed towards $l \approx 290^\circ$ can be ascribed to perturbations of the HI local to Car OB2, and not to a large-scale phenomenon in the Galaxy.

Acknowledgements. One of us (JRR) wish to thank to Dr. E. Bajaja for his guidance during early stages of this research. The timely remarks of the referee, Dr. Y. Georgelin, is greatfully acknowledged. This work was partially supported by the Argentinian National Research Council (CONICET), under project PID 3-0838800/88.

References

Arnal E.M., Cersósimo J.C., May J., Bronfman L. 1987, A&A, 174, 78
Bania T.M., Lyon J.G. 1980, ApJ, 239, 173
van der Bij M.D.P., Arnal E.M. 1986, Astrophys. Lett., 25, 119
Blomme R. 1990, A&A, 229, 513
Blomme R., van Rensbergen W. 1988, A&A, 207, 70
Cappa de Nicolau C.E., Niemela V.S., Dubner G.M., Arnal E.M. 1988, AJ, 96, 1671
Castor J.I., McCray R., Weaver R., 1975, ApJL, 200, L107
Caswell J.L., Haynes R.F. 1987, A&A, 171, 261
Caswell J.L., Robinson B.J. 1974, Aust. J. Phys., 27, 597
Chromey F.R., Elmegreen B.G., Elmegreen D.M. 1989, AJ, 98, 2203
Clariá J.J. 1976, AJ, 81, 155
Fich M., Blitz L., Stark A.A., 1989, ApJ, 342, 272
García B. 1993, ApJS, 87, 197
García B. 1994, ApJ, 436, 705
Georgelin Y.M., Georgelin Y.P. 1976, A&A, 49, 57
Georgelin Y.P., Georgelin Y.M. 1970, A&A, 6, 349
de Geus E.J. 1988, Ph. D. Thesis, Univ. of Leiden
Goss W.M., Shaver P.A. 1970, Aust. J. Phys., 14,1
Grabelsky D.A. 1986, NASA Tech. Memo. 87798
Grabelsky D.A., Cohen R.S., Bronfman L., Thaddeus P. 1988, ApJ, 331, 181
Grabelsky D.A., Cohen R.S., Bronfman L., Thaddeus P., May J. 1987, ApJ, 315, 122
Howarth I.D., Prinja R.K. 1989, ApJS, 69, 527
Humphreys R.M. 1972, A&A, 20, 29
Humphreys R.M., Kerr F.J. 1974, ApJ, 194, 301
Kerr F.J., Bowers P.F., Jackson P.D., Kerr M. 1986, A&AS, 66, 373
Klare G., Neckel Th. 1977, A&AS, 27, 215
Koo B.-C., McKee C.F. 1992, ApJ, 388, 93
Lamers H.J.G.L.M., Leitherer C. 1993, ApJ, 412, 771
Leitherer C., Robin C., Drissen L. 1992, ApJ, 401, 596
Lodén L.O., Lodén K., Nordström B., Sundman A., 1976, A&AS, 23, 283
Manchester R.N., Robinson B.J., Goss W.M. 1970, Aust. J. Phys., 23, 751
Mathewson D.S., Healey J.R., Rome J.M. 1962, Aust. J. Phys., 15, 354
McCray R. 1982, High. of Astron., 6, 565
McCray R., Kafatos M. 1987, ApJ, 317, 190
McKee C.F., Van Buren D., Lazareff B. 1984, ApJL, 278, L115
Moffat A.F.J., Vogt N. 1975, A&AS, 20, 125
NRAO 1992, Images from the Radio Universe (CD-ROM version)
Rizzo J.R. 1994, Ph. D. Thesis, Univ. of La Plata
Rizzo J.R., Bajaja E. 1994, A&A, 289, 622
Robinson B.J., Caswell J.L., Goss W.M. 1974, Aust. J. Phys., 27, 575
Sancisi R. 1974, IAU Symp., 60, 115
Schaller G., Schaerer D., Meynet G., Maeder A. 1992, A&AS, 96, 269
Schmidt-Kaler Th. 1982, Numerical Data and Functional Relationships in Science and Technology. New Series, Group VI, vol. 2b, Landolt-Bornstein, Springer-Verlag, Berlin
Seggewiss W. 1970, IAU Symp., 38, 265
Shaver P.A., Goss W.M. 1970, Aust. J. Phys.Suppl., 14, 133
Simonson S.C., van Someren Greve H.W. 1976, A&A, 49, 343
Smith E. van P. 1965, ApJ, 124, 43
Snow Th.P. 1982, IAU Symp., 98, 377
Steppe H. 1977, A&AS, 27, 415
Strong A.W., Riley P.A., Osborne J.L., Murray J.D. 1982, MNRAS, 201, 495
Thomas B.M., Day G.A. 1969, Aust. J. Phys. Suppl., 11, 3
Vacca W.D., Garmany C.D., Shull J.M. 1996, ApJ, 460, 914
Van Buren D. 1985, ApJ, 294, 567
Van Buren D. 1986, ApJ, 306, 538
Walborn N., 1973, AJ, 78, 1067
Weaver R., McCray R., Castor J., Shapiro P., Moore R. 1977, ApJ, 218, 377
Wilson T.L., Mezger P.G., Gardner F.F., Milne D.K. 1970, A&A, 6, 364

This article was processed by the author using Springer-Verlag LaTeX A&A style file *L-AA* version 3.